Ultra-broadband optical spectrum generation from a stretched pulse fiber laser utilizing zero-dispersion fiber

Cheng Zhang (张 程)*, Lu Chai (柴 路), Youjian Song (宋有建), Minglie Hu (胡明列), and Chingyue Wang (王清月)

Ultrafast Laser Laboratory, Key Laboratory of Opto-electronic Information Technical Science of Ministry of Education, College of Precision Instruments and Opto-electronics Engineering, Tianjin University, Tianjin 300072, China

**Corresponding author: cheng_zhang_2010@163.com*

Received December 25, 2012; accepted January 27, 2013; posted online April 19, 2013

We investigate the effects of a piece of zero-dispersion fiber (ZDF) on the pulse dynamics of a passively mode-locked fiber laser operating in the stretched-pulse regime. Numerical simulation suggests that the proper location and length of ZDF facilitate spectrum broadening and pulse shortening in fiber lasers while maintaining constant net cavity dispersion. A nonlinear polarization evolution mode-locked Er-doped fiber laser with a dispersion map is built based on the simulation. Larger optical spectrum broadening is obtained by inserting a longer ZDF after the active fiber during single-pulse operation, which well agrees with the simulation.

OCIS codes: 140.3500, 140.3510, 140.4050, 320.7090.
doi: 10.3788/COL201311.051403.

Fiber lasers are interesting because of their compact size, low cost, and high stability. Meanwhile, the generation of ultrashort pulses with a broadband optical spectrum is attracting considerable attention in the fields of frequency metrology[1], high precision optical sampling[2], and bio-imaging[3]. An ultra-broadband spectrum with extremely low linewidth is required especially for optical frequency comb-based metrology, precision spectroscopy[4], or applications for extreme nonlinear optics[5]. Zero-dispersion fiber (ZDF) lasers can generate ultrashort, broad bandwidth pulses with extremely low spectral line phase noise[6], which is ideal for coherent spectral comb generation with low linewidth.

Zhao *et al.*[7] reported the generation of 120-nm-bandwidth noise-like pulses in a passively mode-locked Er-doped fiber (EDF) ring laser under soliton operation by inserting a segment of slightly normal-dispersion fiber within the cavity. However the pulse train quality is low. In 2009, Deng *et al.*[8] showed the direct generation of 55-fs pulses with 61-nm spectrum width from an all-fiber Er-doped ring laser oscillator using nonlinear polarization rotation mode-locking. In 2010, Ma *et al.*[9] realized 37.4-fs pulse generation from a ring-cavity EDF laser in the stretched-pulse regime at a repetition rate of 225 MHz. The spectral bandwidth of the pulses is 135 nm, and the single-pulse energy is 0.31 nJ. Nikodem *et al.*[10] achieved 111-fs pulses with a fundamental repetition rate of 169 MHz using an all-fiber configuration. In 2012, Chong *et al.*[11] demonstrated broad-spectrum ($\sim$200 nm) pulse generation without gain-bandwidth limitation using a normal-dispersion laser. They found that the pulse can be dechirped to $\sim$20 fs.

In this work, we propose a method of inserting a segment of ZDF into an EDF laser to enable intracavity spectrum broadening while maintaining cavity dispersion in the vicinity of the zero-dispersion region. Consequently, we obtain the accumulation of nonlinearity for spectral broadening and pulse shortening without inducing large net cavity dispersion that can result in a long pulse duration and high spectral linewidth phase noise. In the simulation, we model the propagation dynamics of pulses through each fiber segment in the cavity. We also analyze the optimum location and length of the ZDF in the cavity for optical spectrum broadening. A nonlinear polarization evolution (NPE) mode-locked Er-doped ring-cavity laser is built based on a cavity design obtained from numerical simulation. The optical spectrum broadening well agrees with the simulations.

The numerical model of the NPE mode-locked fiber laser with ring cavity configuration is shown in Fig. 1. The cavity is composed of an active fiber, a single-mode fiber (SMF) (OFS, 980 nm) for a wavelength division multiplexer (WDM), two segments of SMFs (SMF28), a saturable absorber (SA), and an output coupler (OC). A piece of ZDF is inserted inside the laser cavity to study the pulse dynamics of pulse shortening and optical spectrum broadening. The effect of different ZDF lengths and positions (marked as 1 and 2, respectively, in Fig. 1) on optical spectral broadening is discussed.

The pulse evolution in the laser cavity is investigated by the complex cubic Ginzburg–Landau equation (CGLE), which can be written as

$$\frac{\partial A(t,z)}{\partial z} = \mathbf{i}\gamma\left|A(t,z)\right|^2 A(t,z) + \frac{1}{2}\left(g-\alpha\right)A(t,z) - \frac{\mathbf{i}}{2}\left(\beta + \mathbf{i}gT_2^2\right)\frac{\partial^2 A(t,z)}{\partial t^2}, \quad (1)$$

where $A(t,z)$ is the slowly varying envelope of the electric field amplitude, z is the propagation parameter, t is

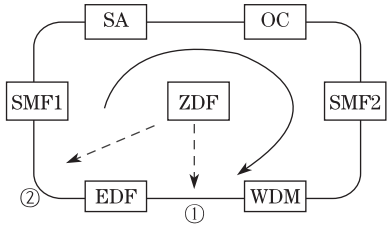

Fig. 1. (Color online) Schematic of the designed fiber laser.

the time scaled to the pulse duration, g is the gain, β is the group velocity dispersion (GVD), γ is the nonlinear parameter, α is the loss, and T_2 is the dipole relaxation time that is inversely proportional to the gain bandwidth. The gain bandwidth is 50 nm, which is typical for EDF lasers. The gain saturation with the total energy is given as $g = g_0/(1+E/E_{\rm sat})$, where g_0 is the small-signal gain, $E_{\rm sat}$ is the gain saturation energy, and E is the instantaneous pulse energy.

In the laser cavity, the NPE mode-locking mechanism is initiated and sustained by an equivalent fast SA. The function of the SA is close to the sinusoidal transmission curve of the nonlinear polarization evolution and modeled by the transmission equation[12]

$$T = 1 - \frac{l_0}{1 + P/P_{\rm sat}}, \tag{2}$$

where l_0 is the unsaturated loss, P is the instantaneous pulse power, and $P_{\rm sat}$ is the saturation power.

Modeling is performed by solving the CGLE using a standard split-step Fourier algorithm. In the first simulation, the schematic cavity is a conventional mode-locked fiber ring laser (Fig. 1) composed of four fiber elements, namely, $L_{\rm WDM}$, $L_{\rm SMF1}$, $L_{\rm SMF2}$, and $L_{\rm Er}$. $L_{\rm WDM}$ is the fiber length of the pump/laser combined port of WDM, which is 15 cm, with $\beta_{\rm WDM} \approx 0$ ps^2/m. $L_{\rm SMF1}$ and $L_{\rm SMF2}$ (31 and 6 cm, respectively) are the pigtails of the fiber minicollimators, with $\beta_{\rm SMF}$=0.022 ps^2/m. $L_{\rm Er}$ is a 40-cm gain fiber, with $\beta_{\rm Er}$=–0.012 ps^2/m. The net dispersion of the cavity is –0.0033 ps^2. The output port and SA are placed between two SMF segments.

The simulated dynamics of pulse evolution in the time and optical spectrum domains within the laser are shown in Fig. 2. The transform-limited pulse durations have two positions inside the cavity: one inside the EDF and the other inside the SMF1 (pulse durations of 132.9 and 65.5 fs, respectively). The laser operates in the stretched-pulse regime with a stretching ratio of 2.66. The pulse spectrum also varies to some extent in the cavity (Fig. 2(b)), which can be explained by the interaction among self-phase modulation (SPM) spectral broadening, gain filtering of limited gain bandwidth, and initial chirp. The effects are balanced at the position corresponding to the maximum spectral width achieved in SMF1, where the shortest transform-limited pulse is located.

In the second simulation, we study the effects of the position and length of the ZDF segment inserted into the aforementioned laser on the pulse dynamics with the other parameters fixed. Firstly, we select two available insertion sites (labeled 1 and 2 in Fig. 1) to investigate the effect of the ZDF position. Figure 3 illustrates the pulse evolution versus the ZDF position in the frequency and time domains during one round trip in the cavity. The red and blue curves represent the position maps when the ZDF is inserted before (labeled 1 in Fig. 1) and after (labeled 2 in Fig. 1) the EDF respectively. The position map without the ZDF is also shown (black curve in Fig. 3) for comparison with the first simulation, i.e., the conventional stretched pulse laser. Analysis of the three curves in Fig. 3(a) reveals that pulse dynamics is very sensitive to the ZDF position. The largest spectrum broadening of 92.18 nm is obtained only inside SMF1 (point A) throughout the cavity when a 70-cm ZDF is placed after gain fiber. By contrast, only a slight change is observed in the other two cases. The reason is that the ZDF induces more SPM-induced spectrum broadening without broadening the pulse duration in the time domain. Furthermore, a large pulse peak power is obtained when placing the ZDF at an optimum location (position 2 in Fig. 1) that facilitates spectrum broadening. Consequently, the shortest transform-limited pulse duration of 47.87 fs is achieved (point B in Fig. 3(b)). This finding can be due to the fact that the abnormal dispersion in SMF compensated for the positive chirp and enabled balance to be achieved.

Apart from altering the position of the ZDF, we also adjust its inserted length to determine the influence on pulse dynamics and output characteristics. We consider only the case of the ZDF placed after the EDF. The results in Fig. 4 show that the maximum spectral bandwidth within the whole cavity monotonically increases with increased embedded ZDF length from 0 to 70 cm (Fig. 4(a)) caused by increased SPM-induced spectrum broadening. Given that the ZDF length is scaled above 70 cm,

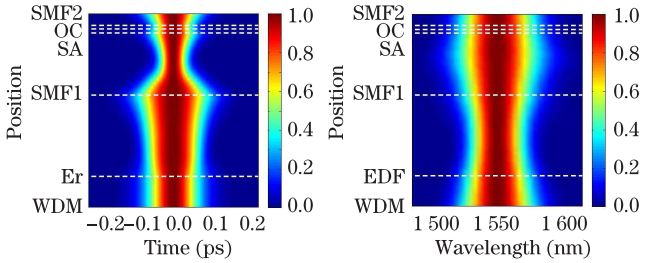

Fig. 2. (Color online) Simulation of the pulse dynamics of the mode-locking fiber laser operating in the vicinity of the zero-dispersion regime: pulse evolution of one round trip (a) in the time domain and (b) in the frequency domain.

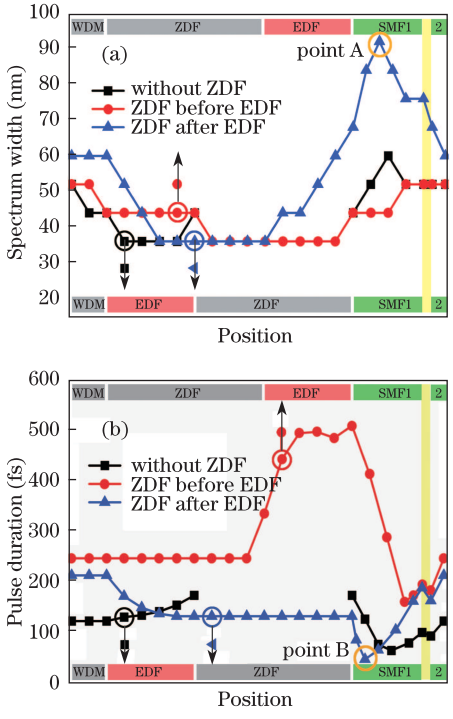

Fig. 3. (Color online) Laser performances versus the intracavity positions of the ZDF: pulse evolution (a) in the frequency domain and (b) in the time domain.

pulse splitting occurs because of the excessive accumulation of nonlinear phase shifts exerted by the SPM effect. Under single-pulse operation, the corresponding shortest transform-limited pulse duration decreases with increased ZDF length (Fig. 4(b)).

To validate the numerical simulation results of optical spectral broadening properties, a corresponding Er-doped passively mode-locked fiber laser operating in the stretched-pulse regime is built. The experimental configuration of the fiber laser and dispersion map is shown in Fig. 5. The fiber is composed of a 40-cm heavily EDF (Liekki 110-4/125), a 15-cm fiber for the WDM, and two pigtails for two minicollimators (SMF28, 31- and 7-cm). Except for the EDF, all other fibers exhibit abnormal dispersion. The group-delay dispersion (GDD) of the WDM fiber and SMF are –0.0013 and –0.022 ps^2/m, respectively, whereas the GDD of the EDF is 0.012 ps^2/m. Therefore, the net cavity dispersion is – 3 535 fs^2 at the central wavelength of 1 550 nm. The total optical cavity length is approximately 114 cm,

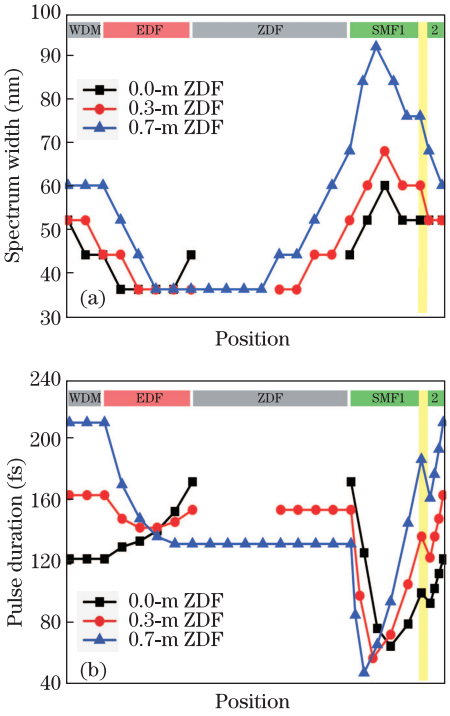

Fig. 4. (Color online) Laser performances versus the intracavity position with increased ZDF length: pulse evolution (a) in the frequency domain and (b) in the time domain.

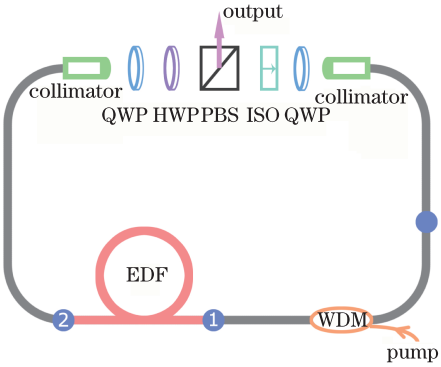

Fig. 5. Schematic of the experimental fiber laser.

resulting in a fundamental repetition rate of 194 MHz. The mode-locking mechanism is initialized and stabilized by the NPE process using two quarter waveplates (QWPs), a half waveplate (HWD), and a polarization beam splitter (PBS). The PBS rejection port also works as the output coupler.

Mode-locking is a self-starting, turnkey operation as long as the pump power reaches the threshold of 345 mW. With the maximum pump power P_p = 700 mW, an average output power of 132 mW corresponding to a pulse energy of 0.68 nJ can be obtained. Mode-locking is stable and can operate for hours without disturbance. The laser is immune to slight fiber movements or vibrations. However, NPE mode-locked lasers are sensitive to temperature changes. Thus, mode-locking does not self-start with large variations in room temperature. However, mode-locking can be rebuilt by slight waveplate rotation.

Using a typical stretched-pulse fiber laser, we experimentally assess the influences of the ZDF on spectral broadening by embedding a specific ZDF segment with different lengths at various positions. The GVD of the OFS 980-nm fiber at 1 550 nm wavelength is –0.0013 ps^2/m, which is 17 times smaller than that of the SMF. Therefore, we adopt this type of fiber to represent the ZDF used to investigate the output performances. The output port is matched with the relative position in the simulation mode (yellow line in Figs. 3 and 4). The overall output characteristics of the modified fiber laser are summarized in Fig. 6.

Based on Fig. 6, a comparison between the output characteristics of the two cases, i.e., ZDFs before and after the EDF with different ZDF lengths, is made. The comparison reveals that a full-width at the 10 dB maximum bandwidth of 172 nm can be obtained when a 70-cm ZDF is placed after the EDF. The corresponding shortest transform-limited pulse width is 36 fs. As revealed by this series of experiments, placing the ZDF after the EDF (position 2 in Fig. 5) leads to a wider optical spectrum at the output port, which agrees with the simulation (Fig. 3(a)). Under this condition, the obtained ptical spectral width is directly proportional to the ZDF length, which increases from 0 to 0.7 m. In addition, the measured autocorrelation traces in Fig. 6(b) indicate that a longer pulse duration is achieved whether ZDF is spliced before or after the EDF. Apparently, the direct output pulse duration also increases with increased ZDF length, which can be observed in Fig. 6(d). The same trend is shown in the numerical results presented in Fig. 4(d). Extracavity dispersion compensation is desirable to further demonstrate the o validity of the optimum fiber lasers with shorter pulse durations. Notably, the laser is not outputted from the maximum spectral bandwidth position. In the next step, we study the optimized output position by simulation and experiments to produce directly a transform-limited pulse duration with the widest optical spectrum.

In conclusion, we numerically and experimentally investigate the effects of the ZDF position and length on the dynamics of pulses propagating through a stretched-pulse fiber laser in the vicinity of zero cavity dispersion. The ZDF location and length are optimized to achieve the largest bandwidth and shortest pulse duration. The

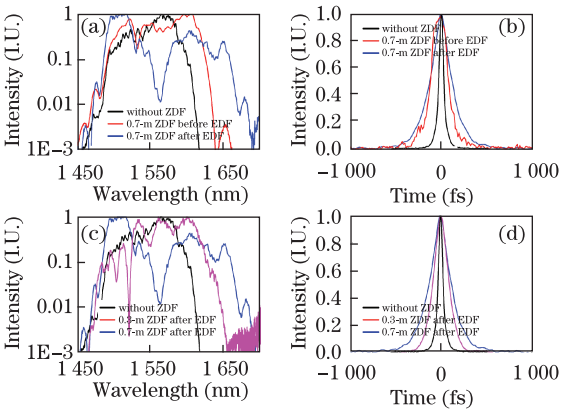

Fig. 6. (Color online) Output pulse spectrum (left) and intensity autocorrelations (right) for varied ZDF positions and lengths. (a) Pulse spectrum and (b) pulse duration with the ZDF position of before (red) and after (blue) the EDF; (c) pulse spectrum and (d) pulse duration with increased ZDF length.

results indicate that optimum laser operation can be realized when the ZDF is located immediately after the gain fiber, whereas a longer fiber length is more suitable for spectral broadening under the limitation of single-pulse operation. The experimental results agree with the numerical simulation results. This work suggests that a section of pure nonlinearity with amount and intracavity position can effectively extend the output pulse to achieve a broader spectrum and shorter pulse duration in stretched-pulse fiber lasers.

This work was supported by the National Key Basic Research Special Foundation of China (Nos. 2011CB808101 and 2010CB327604), the National Natural Science Foundation of China (Nos. 60838004, 60678012, 60978022, 61078028, 61205131, and 11274239), the New Century Excellent Talents (No. NCET-07-0597), the Doctoral Program Foundation of Institution of Higher Education of China (No. 20090032110050), and the National "111" Project of China (No. B07014).

References

1. S. T. Cundiff, Nature **450,** 1175 (2007).
2. A. Bartels, R. Cerna, C. Kistner, A. Thoma, F. Hudert, C. Janke, and T. Dekorsy, Rev. Sci. Instrum. **78,** 351071 (2007).
3. F. Lu, W. Zheng, J. Lin, and Z. W. Huang, Appl. Phys. Lett. **96,** 133701 (2010).
4. A. Marian, M. C. Stowe, J. R. Lawall, D. Felinto, and J. Ye, Science **306,** 2063 (2004).
5. G. G. Paulus, F. Grasbon, H. Walther, P. Villoresi, M. Nisoli, S. Stagira, E. Priori, and S. Desilvestri, Nature **414,** 182 (2001).
6. L. N. Glandorf, T. A. Johnson, Y. Kobayashi, and S. A. Diddams, Opt. Lett. **36,** 1578 (2011).
7. L. M. Zhao, D. Y. Tang, T. H. Cheng, H. Y. Tam, and C. Lu, Opt. Commun. **281,** 157 (2008).
8. D. Deng, L. Zhan, Z. Gu, Y. Gu, and Y. Xia, Opt. Express **17,** 4284 (2009).
9. D. Ma, Y. Cai, C. Zhou, W. J. Zong, L. L. Chen, and Z. G. Zhang, Opt. Lett. **35,** 2858 (2010).
10. M. Nikodem and K. Abramski, Opt. Commun. **283,** 109 (2010).
11. A. Chong, H. Liu, B. Nie, B. G. Bale, S. Wabnitz, W. H. Renninger, M. Dantus, and F. W. Wise, Opt. Express **20,** 14213 (2012).
12. A. Chong, W. H. Renninger, and F. W. Wise, J. Opt. Soc. Am. B **25,** 140 (2008).